



MobileSense: Tracking Air Pollution Exposure of Frontline Motorcycle Riders Using a Mobile Low-Cost Sensor Platform

Raunak Mukhia

intERLab

Asian Institute of Technology

Pathumthani, Thailand

rmukhia@ait.ac.th

Kalana G.S. Jayarathna

intERLab

Asian Institute of Technology

Pathumthani, Thailand

kalana@ait.ac.th

Ratchaphon Samphutthanont

AiroTEC

Chiang Mai Rajabhat University

Chiang Mai, Thailand

ratchaphon_sam@cmru.ac.th

Adisorn Lertsinsrubtavee

intERLab

Asian Institute of Technology

Pathumthani, Thailand

adisorn@ait.ac.th

Nussara Tieanklin

University of Washington

Seattle, USA

nussara@cs.washington.edu

Preechai Mekbungwan

intERLab

Asian Institute of Technology

Pathumthani, Thailand

preechaim@ait.ac.th

Joseph Breda

University of Washington

Seattle, USA

joebreda@cs.washington.edu

Kurtis Heimerl

University of Washington

Seattle, USA

kheimerl@cs.washington.edu

Thongchai Kanabkaew

Thammasat University

Rangsit, Thailand

thongchai.k@fph.tu.ac.th

Kanchana Kanchanasut

intERLab

Asian Institute of Technology

Pathumthani, Thailand

kanchana.kanchanasut@cs.ait.ac.th

CCS Concepts

- Human-centered computing → *Ubiquitous and mobile computing systems and tools.*

Keywords

Air Pollution Monitoring, PM_{2.5} exposure, Health Risk Assessment, low-cost mobile sensing, Internet of Things

ACM Reference Format:

Raunak Mukhia, Adisorn Lertsinsrubtavee, Preechai Mekbungwan, Kalana G.S. Jayarathna, Nussara Tieanklin, Joseph Breda, Ratchaphon Samphutthanont, Thongchai Kanabkaew, Kurtis Heimerl, and Kanchana Kanchanasut. 2025. MobileSense: Tracking Air Pollution Exposure of Frontline Motorcycle Riders Using a Mobile Low-Cost Sensor Platform. In *ACM SIGCAS/SIGCHI Conference on Computing and Sustainable Societies (COMPASS '25), July 22–25, 2025, Toronto, ON, Canada*. ACM, New York, NY, USA, 14 pages. <https://doi.org/10.1145/3715335.3735496>

1 Introduction

Urban air pollution, particularly fine particulate matter (PM_{2.5}), poses a significant public health threat in rapidly developing cities such as Bangkok [2, 13, 15] and Chiang Mai [17]. In recent years, these cities have commonly experienced PM_{2.5} levels exceeding safe thresholds, endangering millions of residents. Prolonged exposure to such pollutants has been linked to severe health risks, including respiratory diseases, cardiovascular conditions, and reduced life expectancy. While policy measures such as work-from-home

Abstract

Air pollution, particularly PM_{2.5}, poses significant health risks to outdoor workers in urban areas like Bangkok and Chiang Mai, yet their actual exposure remains poorly understood. Traditional fixed-site monitors often underestimate actual exposure levels. To address this, we introduce MobileSense, a low-cost mobile air quality monitoring platform that provides real-time PM_{2.5} data using a helmet-mounted sensor system with GPS tracking and alerts. A seven-month field study revealed that front line motorcycle riders experience significantly higher PM_{2.5} exposure than recorded by fixed monitors, exceeding WHO safety limits, even in the non polluted season. Health risk assessment using the Hazard Quotient (HQ) method classified 6 out of 10 riders as high-risk. To mitigate exposure, we evaluated three strategies: (1) a daily 1-hour break, (2) full days off on consecutive high-pollution days, and (3) full days off on peak pollution days. Bangkok riders benefit more from hourly breaks during rush hours, while Chiang Mai riders benefit more from full days off due to consistently high pollution levels. Our findings highlight the need for targeted exposure reduction strategies and provide valuable insights for protecting outdoor workers from air pollution.



This work is licensed under a Creative Commons Attribution 4.0 International License.
COMPASS '25, Toronto, ON, Canada

© 2025 Copyright held by the owner/author(s).

ACM ISBN 979-8-4007-1484-9/25/07

<https://doi.org/10.1145/3715335.3735496>

(WFH) initiatives have been introduced to minimize pollution exposure, these benefits are largely limited to white-collar professionals. Outdoor workers, such as food delivery riders, street cleaners, and motorcycle taxi drivers, remain highly vulnerable with no alternative but to endure prolonged exposure to hazardous air conditions. Despite their increased health risks, real-time personal exposure data for these groups remain scarce, representing a critical gap in current air pollution research and mitigation efforts.

Fixed-site air quality monitoring, even with low-cost sensor networks [20, 23], are usually sparse and need an algorithmic approach [13] or simulation [15] to estimate and approximate fine-grained spatial variations in pollution levels. A recent study by [19] indicates that outdoor ($PM_{2.5}$) concentrations are consistently higher than indoor levels, placing outdoor workers at high risk of exposure to harmful particulate matter. This discrepancy underscores the need for more precise exposure assessments, particularly for individuals who spend prolonged hours outdoors and whose real-world pollution exposure is often underestimated by traditional air quality monitoring frameworks.

In this paper, we introduce MobileSense, a low-cost, mobile air quality sensor platform designed for motorcycle riders. Mounted on a rider's helmet, MobileSense continuously monitors air pollution exposure and GPS location in real-world conditions. The platform integrates with a real-time dashboard that tracks pollution levels on the move and includes an alert system to warn riders of hazardous air quality or sensor malfunctions. To demonstrate its feasibility, we conducted a seven-month field study with volunteer riders in Bangkok and Chiang Mai, Thailand. We analyzed the collected data to assess actual pollution exposure in both cities, comparing the levels with WHO-recommended safety limits. Finally, we performed a health risk assessment for each rider and proposed mitigation strategies, such as taking short breaks during the day or full days off, to minimize long-term exposure risks. The findings from this study will provide critical insights into occupational air pollution risks and inform policies aimed at protecting outdoor workers from long-term health impacts.

2 Related Work

With the advent of mobile sensors, researchers have performed extensive work to study spatial, temporal, and personal exposure to pollutants like $PM_{2.5}$. Studies using mobile sensors have been conducted using specialized vehicles or fixed routes. Apté et al. [6] conducted a year-long study using Google Street View vehicles equipped with reference-grade air quality sensors (NO , NO_2 and black carbon) to generate annual daytime pollution maps with a 30-meter spatial resolution. Similarly, Ghaida et al. [14] collected street level $PM_{2.5}$ data at 1-second intervals using Google Street View cars in Jakarta, Indonesia, revealing correlations between air quality disparities and socioeconomic factors in eight neighborhoods. Meanwhile, DeSouza et al. [12] mounted low-cost sensors on municipal trash trucks to monitor $PM_{2.5}$ concentrations, identifying pollution hotspots and characterizing emission sources by analyzing median pollutant levels along 30-meter road segments. However, these existing approaches have limitations when studying the occupational exposure patterns of outdoor workers, particularly food delivery drivers on motorcycles, whose routes and schedules

are inherently unpredictable. In addition, motorcycle riders lack access to power terminals, requiring portable power supplies and energy-efficient sensors.

Behr et al. [9] developed a smart helmet equipped with air quality and hazardous event detection for the mining industry. The system is capable of detecting dangerous levels of hazardous gases, helmet removal by miners, and collision or impact events. Alim et al. [5] designed a smart helmet for motorcyclists that integrates an alcohol detection system. This system prevents an intoxicated driver from starting the engine and notifies a designated contact in the event of an accident, improving safety on the road. Although similar to our work, which utilizes the helmet-based approach, these systems rely on Zigbee to transmit dangerous events and GSM text messages for accident notifications, which are unsuitable for applications requiring frequent sensor data transmission.

Large-scale initiatives further demonstrate the potential of mobile sensing for city-wide pollution mapping. Liu et al. [31] deployed 125 electric taxis equipped with CO_2 , NO_2 , and $PM_{2.5}$ sensors over 13 months, achieving 80% coverage of major roadways and enabling pollution mapping at a resolution of 200 meters. A study by Aswin et al. [16] evaluated the spatiotemporal exposure of auto-rickshaw drivers to PM pollution. Using a mobile monitoring setup in an auto-rickshaw, PM_{10} , $PM_{2.5}$, and PM_1 concentrations were measured during peak and non-peak weekday hours across 15 administrative zones. However, given our study's limited number of participants and extended duration, a single sensor malfunction could result in significant data loss, highlighting the need for real-time data collection through a cellular network that can monitor sensor health. Furthermore, physically requiring participants to collect data from sensor loggers would interfere with their daily work routines. To address these challenges, we implemented an automated notification system that alerts participants when their sensors malfunction, enabling immediate corrective actions such as sensor restart. Our modular sensor system design also allows targeted replacement of malfunctioning components. These improvements enable long-term sensor deployment with minimal participant involvement while continuously monitoring sensor health.

Mobile sensing has also been applied to assess personal exposure. Win-Shwe et al. [33] tracked real-time $PM_{2.5}$ exposure for 30 middle-aged participants using GPS-enabled Pocket $PM_{2.5}$ sensors during their daily activities. Although promising with its 1 Hz data collection rate and portability, the system lacks real-time data collection capabilities.

A study by Sun et al. [18] investigated the accuracy and effectiveness of real-time personal $PM_{2.5}$ monitoring using low-cost sensors compared to fixed-station monitoring for asthmatic children in the study area. Forty-seven children carried a low-cost sensor (PICO) that measured $PM_{2.5}$, temperature, and humidity every 5 minutes, alongside GPS location. These data were compared with hourly $PM_{2.5}$ data from the nearest fixed monitoring station. The commercial portable sensor used in the study lacks cellular capability, which limits city-wide real-time data collection.

Although some studies in Bangkok and Chiang Mai have explored health outcomes associated with exposure to air pollution, they often rely on static monitoring data rather than individualized, high-resolution exposure measurements. Ahmad et al. [2] have carried out a health risk assessment in Bangkok using data from three

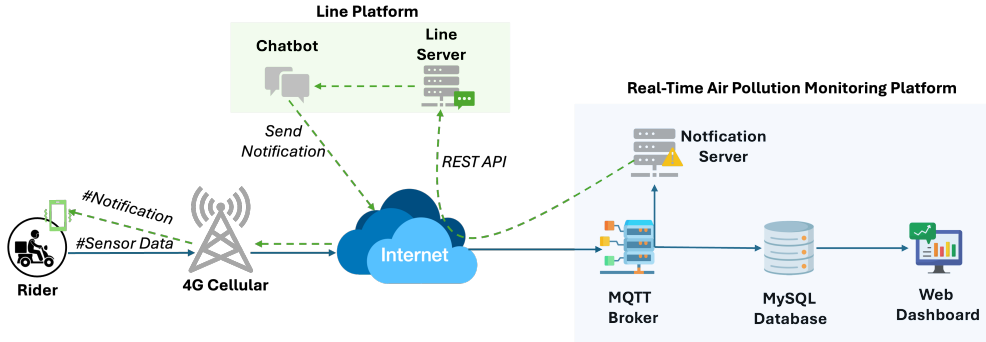


Figure 1: System Architecture

static reference sensors in Ari, Din Daeng, and Bangna, without involving participants. Kausar et al. [17] have conducted studies to determine the impact of PM_{2.5} on ocular health of 50 individuals using data obtained from the Northern Thailand Air Quality Index (NTAQI) as the baseline. In contrast, our system combines mobile sensing with continuous, participant-specific exposure monitoring, enabling more accurate characterization of individual health risks in real-world occupational settings.

3 MobileSense's Architecture

The system architecture of MobileSense, shown in Figure 1, is designed to collect, process, and share real-time air quality data with high spatial resolution. The architecture is composed of four key components:

- (1) The *Mobile Sensing Node* is mounted on the rider's helmet and collects environmental data such as PM_{2.5} levels along with GPS positioning for precise localization.
- (2) The *Communication Layer* facilitates the transmission of collected data from the mobile sensing unit to the cloud via a cellular network.
- (3) The *Data Processing Unit* is hosted in the cloud and includes an MQTT broker for efficient data transmission, a database for storing the collected data, and a web dashboard for visualizing the information; and
- (4) The *Notification System*, integrated with a messaging service, that alerts the rider in case of any malfunction detected in the mobile sensing unit.

Details of each component are described below:

3.1 Mobile Sensing Node

The design of the mobile sensing node (MSN) requires careful consideration of size, weight, safety, power consumption, airflow, and cost. To accurately measure air pollution inhaled by the rider, we mounted the sensing unit on the rider's helmet. This placement ensures precise exposure measurements while keeping the unit lightweight, secure, and comfortable for extended use.

The MSN consists of three main components: (1) the sensor box, which houses the air quality sensors; (2) the control box, which handles data processing and communication; and (3) the power source, which supplies energy to the entire system.

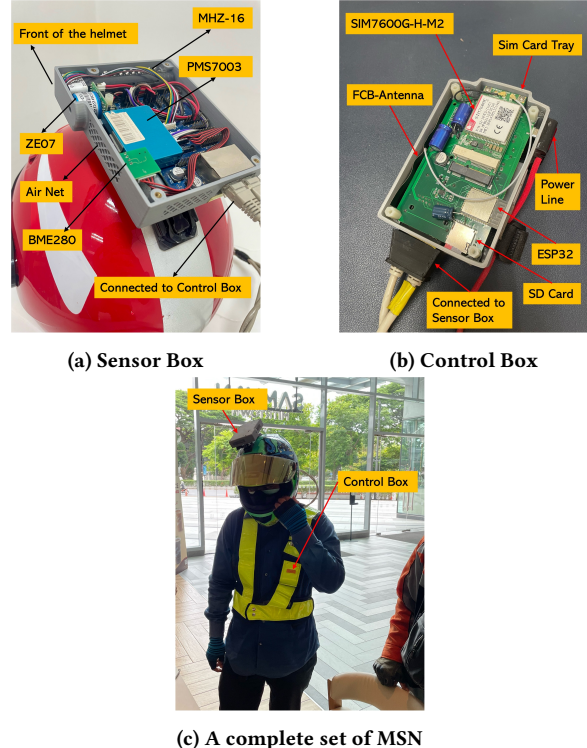


Figure 2: The hardware design of the Mobile Sensing Node (MSN) includes the sensor control box (a), the control box (b), and (c) a complete MSN setup attached on the rider while the control box attached the vest jacket.

3.1.1 Sensor Box. The sensor box is equipped with multiple air sensors, including those for Particulate Matter (PM₁, PM_{2.5}, and PM₁₀), Carbon Dioxide (CO₂), Carbon Monoxide (CO), Temperature, Humidity and Air Pressure. For particulate matter detection, we selected the Plantower PMS7003 sensor [27] due to its affordability, proven reliability, and excellent unit-to-unit consistency, as confirmed by several studies [7, 8, 10]. The CO₂ and CO sensors were selected from the Winsen brand, specifically the MH-Z16 model [35] for CO₂ and the ZE07 model [34] for CO. Temperature,

humidity and air pressure are measured using the BME280 [29] sensor, chosen for its compact design and low power consumption. The PMS7003, MH-Z16, and ZE07 sensors are connected to the main control unit (MCU) via UART lines through a multiplexer. Meanwhile, the BME280 is connected to the MCU via the I2C line. The orientation of the sensors is shown in the Figure 2a. The PM sensor is placed on the left side of the box, which features a cutout for better ventilation. This cutout is designed with a net-like shape to allow optimal airflow to the sensor while maintaining the strength of the box, protecting the sensor from direct exposure to rain, debris, and impacts, ensuring accurate air quality measurement.

The sensor box is connected to the control box housing the MCU through two RJ45 cables, which transmit power, ground, I2C signals, UART communication, analog signals, enable signals, and multiplexer selection signals from the control box to the sensor box. These cables provide a secure and efficient data transfer pathway, ensuring that the sensor data is reliably communicated to the MCU for processing. The sensor box is 3D-printed to achieve a compact design that ensures comfort for the rider. The box measures 50 mm in width, 6 mm in length, and 30 mm in depth, making it both lightweight and ergonomic.

3.1.2 Control Box. Figure 2b illustrates the control box, which manages data collection from all connected sensors, processes the information, and transmits it to the server. At its core is the ESP32-WROOM-32D [32], a cost-efficient, low-power system-on-chip (SoC) microcontroller with an embedded Xtensa dual-core 32-bit CPU running at 160 MHz. For data transmission, the SIM7600G-H-M2 [21] module from SIMCom, a 4G communication module, is selected for its ability to support uplink speeds of up to 50 Mbps. Also the software multiplexing between GNS and Cellular data reduces the bandwidth as they have their overhead. An FCB-type antenna is chosen for its ease of integration inside the control box, ensuring a compact design. Additionally, the SIM7600G-H-M2 module includes GNSS functionality, enabling real-time location tracking alongside air pollution data collection. Figure 2c illustrates the mobile sensing node deployed on a rider. The sensor box is mounted on the helmet, while the control box, is securely placed in a pocket of the rider's vest jacket. The two components are interconnected via an Ethernet cable, ensuring seamless data transmission.

The micro-controller firmware is designed with a modular architecture to ensure efficient and reliable system operation. It includes a Hardware Abstraction Layer (HAL) to provide seamless access to hardware resources, along with a Configuration Manager that oversees system settings and parameters. A Storage Manager, utilizing the FAT32 file system, enables organized data storage on an SD card. The Sensor Manager is responsible for periodic data acquisition, ensuring timely collection of information from all connected sensors. Additionally, the firmware integrates a Network Manager to handle network connectivity and related tasks, while an HTTP Server provides a web-based user interface for system configuration. To support communication in IoT (Internet of Thing) applications, an MQTT Client is included, and an RTC Handler manages real-time clock functionality to ensure accurate timekeeping.

The Sensor Manager operates by collecting data from all attached sensors at a fixed interval of one second. This data is then saved to the SD card, leveraging the Storage Manager for structured storage.

3.1.3 Power Source. The power source is a critical component of our design, as it must provide sufficient capacity while remaining compact and lightweight to ensure portability. Our system needs to operate for approximately 8-10 hours to accommodate the working shifts of each rider. For this reason, we selected a power bank for convenience, allowing easy battery swapping during the day if needed. The air helmet system consumes around 3.5 watt-hours, powered by a 5V supply from the battery. After evaluating the power needs, we opted for a 10,000 mAh battery with a discharge capacity of 36 watt-hours, which is sufficient to support up to 8 hours of operation per day.

3.1.4 Cost. The total cost of a complete MobileSense Node (MSN) unit is approximately 400 USD. The estimated costs are divided as follows: the sensor box, which houses multiple sensors including the PMS7003 [27], MH-Z16 [35], ZE07 [34], and BME280 [29], costs approximately 120 USD. The control box, containing the ESP32-WROOM-32D System-on-Chip (SoC) microcontroller and a 64 GB SD card, is estimated at 50 USD. The 4G communication module and GPS sensor (SIM7600G-H-M2) add approximately 50 USD. The printed circuit board (PCB) and additional electronic components contribute around 100 USD. Finally, the enclosure, fabricated using 3D printing, costs about 80 USD.

Compared to other low-cost sensors on the market, prices typically range from 200 to 500 USD. For example, the PurpleAir Zen sensor costs approximately 300 USD [28], while the AirVisual Outdoor air quality monitor is priced around 420 USD [4]. In our previous project, SEA-HAZEMON [1, 20], we deployed static sensor nodes across both urban and forested areas, with each unit costing approximately 350 USD. The cost of the MobileSense Node is slightly higher, primarily due to the inclusion of a 4G communication module and the custom-fabricated enclosure designed to integrate with a helmet.

The MSN is designed with modularity in mind, allowing it to support various sensor configurations depending on the application's requirements and budget. This flexibility makes the system scalable and cost-efficient for different deployment scenarios. For instance, in resource-constrained settings, removing certain sensors such as the CO₂, CO, or BME280 modules can reduce the overall cost.

3.2 Communication Protocol

To efficiently collect and transmit data from our mobile sensing nodes, the Message Queuing Telemetry Transport (MQTT) [22] protocol is used due to its low bandwidth requirements and reliable message delivery. The control box establishes and maintains a persistent connection to an MQTT broker hosted on a cloud server, using the lightweight MQTT client library provided by Espressif Systems, the manufacturer of the micro-controller used in the system.

The Network Manager reads the data from the SD card, formats it into JSON object, and publishes it to a predefined MQTT topic, "air-monitor/*sensor_id*/data", where *sensor_id* represents the unique identifier for the sensor. An MQTT client, operating as a subscriber on the same cloud server as the broker, receives the published JSON data in real time. Upon successful receipt, the subscriber sends an acknowledgment to the sensor on a fixed topic,

"air-monitor/*sensor_id*/ack", containing the timestamp of the collected data. Following this, the data is stored in a MySQL database for further analysis and processing. Once the acknowledgment is received by the sensing node, the corresponding entry on the SD card is deleted to prevent the retransmission of duplicate data.

The data publishing rate matches the data collection rate of 1 packet per second (1 Hz). Each sensor data packet comprises 2 bytes for the fixed MQTT header, 41 bytes for the variable header (topic name) and 430 bytes for the payload, totaling approximately 473 bytes per second at the application layer. However, accurately estimating uplink bandwidth usage requires accounting for TCP and 4G-LTE network overhead.

3.3 Data Visualization

A web-based application was selected for real-time data monitoring and visualization due to its cross-platform capability, allowing users to access monitoring data from any device. Users can easily access the data through a web browser without the need to install additional software. Figure 3 presents an example of our web interfaces for data monitoring and visualization. Figure 3a presents current air quality levels and the location of each user. Users can query data by selecting specific sensor types (e.g. PM_{2.5}, temperature, CO₂) and specifying the date and time of the measurements, as demonstrated in Figure 3b.

The web application offers a user-friendly interface that provides real-time updates on current air quality levels and GPS locations of sensors. As shown in Figure 3, the sensors' locations are shown on the map interface as circles, filled with color, which indicate the concentration of the pollution. Users can also select the date and time duration to explore historical data to identify trends and patterns, aiding in informed decision-making. The interface also allows users to choose data by specific type of sensors (e.g., PM_{2.5}, temperature, CO₂) and timeframes.

The application's backend components, powered by PHP and Python, retrieve sensor data from the MySQL database and process it for presentation on the frontend. The frontend, powered by HTML, JavaScript and Google Maps API, renders the data in an interactive map display, showing sensor locations and data overlays.

3.4 Notification System

Long term measurement may cause the sensor node to malfunction or become unresponsive, leading to data loss. To address this issue, we implemented a notification service that alerts the rider whenever the node goes offline or becomes unreachable. This allows the rider to promptly check the equipment and follow troubleshooting instructions provided by the system.

For notifications, we chose LINE, a widely-used messaging application across many Asian countries, which all our volunteer riders are already familiar with. LINE offers a messaging API [11], allowing us to forward notification messages from our server to the riders. The integration between the notification server and the LINE platform is illustrated in Figure 1. Initially, we created a LINE chatbot and registered it with the LINE server by linking the URL of our notification server as a webhook. The LINE server then issued a valid token to facilitate message exchanges between the chatbot and our notification server.

In our configuration, the notification server continuously monitors sensor data from each rider. If no data is received for more than 2 minutes, a notification is sent to the rider, prompting them to initiate the troubleshooting process. As part of the procedure, riders are advised to wait for 5 minutes after receiving the notification. This delay accounts for potential temporary disconnections, such as those caused by cell site handovers or areas with poor signal coverage, allowing the node to automatically reconnect. The early alert is intentional and important. Not all sensor failures automatically resolve within the 5-minute window. Some problems, such as physical disconnections caused by jerky movements, require manual intervention. A delayed notification in such cases would increase downtime and result in increased data loss. By notifying the rider after just 2 minutes without data, the system emphasizes responsiveness and helps enable faster recovery from persistent failures.

To enhance reliability, the control box firmware is designed to detect and address faulty events. For example, it can automatically reset the network card or reboot the entire system. However, if the node remains offline for more than five minutes without the rider receiving a follow-up notification indicating that the sensor is back online, manual intervention is required. In such cases, riders must manually check their node by following these steps: inspecting the power cable, checking the battery, and performing a hard reset of the node.

4 Performance Evaluation of Low-Cost Sensor

Although low-cost sensors are typically pre-calibrated by the manufacturer, these calibrations are often generic and may not account for the specific environmental conditions in different regions. Factors such as temperature, humidity, and the presence of other pollutants can significantly affect sensor performance. Therefore, field calibration against high-precision reference instruments is crucial to maintain accuracy over time. In line with this, we followed the microsensors challenge protocol [3], ensuring that each sensor node was thoroughly tested in a real-world ambient environment by co-locating them with a reference air quality station owned by the Pollution Control Department of Thailand (PCD). The station locates in the downtown area of Bangkok, utilizes the beta ray attenuation method [30] to measure PM_{2.5} concentrations, providing hourly averages for comparison.

Figure 4 shows a time series of hourly average PM_{2.5} readings from the reference air quality station (PCD) alongside data from low-cost sensors over a 5-day measurement period (117 hours). The readings from the low-cost sensors display a strong correlation with those from the PCD station, with Pearson correlation coefficients (r) consistently above 0.81, indicating a very strong positive linear relationship. This high correlation suggests that the low-cost sensors effectively track PM_{2.5} concentration changes in alignment with the reference station, with only minor discrepancies. The slight elevation in low-cost sensor readings may reflect their higher sensitivity. Figure 5 presents scatter plots comparing PM_{2.5} readings from the PCD station and low-cost sensors 101, 102, 103, and 104, showing correlation coefficients (r) of 0.8159, 0.8164, 0.8153, and 0.8137, respectively

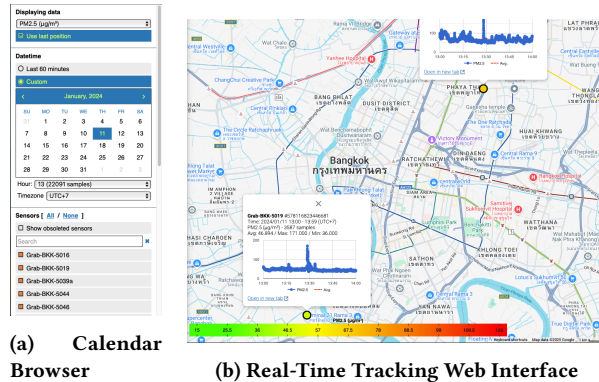


Figure 3: The web application interface of MobileSense. (a) shows calendar browser for retrieving historical data, (b) shows the main web interface displays sensor data and location in both real-time and historical view

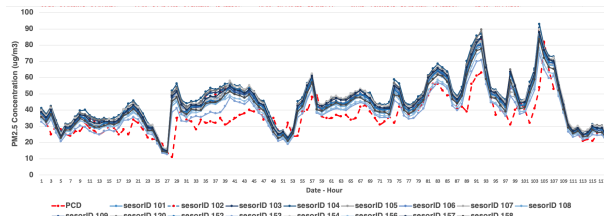


Figure 4: Comparison between PM_{2.5} concentration readings from the reference station (PCD) and low-cost sensors.

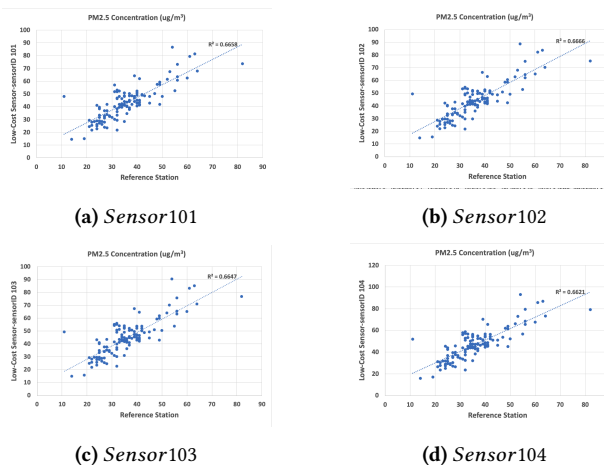


Figure 5: Scatter plots comparing PM_{2.5} readings from low-cost sensors and air quality reference station

5 Experimental Design

To evaluate the sensor designs, we conducted a deployment in two major cities in Thailand: Bangkok and Chiang Mai. Prior to the experiment, we set up static monitoring stations on buildings and roadside units in central areas of each city. The static sensors operated on wall power and utilized WiFi connectivity instead of battery power and cellular data. A total of nine sensors were

deployed in Bangkok and three in Chiang Mai. These static nodes were equipped with the same sensors as the Mobile Sensing Node (MSN) to ensure unbiased comparisons. Figures 6a and Figure 6b illustrate the study areas in Bangkok (1,571.4 km²) and Chiang Mai (721.8 km²), with cross-mark icons indicating the locations of our static sensors.

In parallel, we recruited motorcycle riders working in taxi or parcel delivery services, as they are among the most exposed to air pollution. Recruitment was carried out through social media messaging platforms and by directly requesting rides via motorcycle taxi applications. The primary criteria for recruitment was working at least five hours a day. Those who did not meet these criteria were excluded from the study. Ultimately, we successfully enlisted 10 riders (5 in Bangkok and 5 in Chiang Mai). Table 1 shows the demographics of the participants.

DriverID	Source of Income	Income Avg/Day (THB)
BKK1	Rideshare, Legacy	2250
BKK2	Legacy	800
BKK3	Rideshare, Legacy	1300
BKK4	Rideshare, Legacy	1350
BKK5	Rideshare	1800
CMI1	Rideshare	700
CMI2	Rideshare	700
CMI3	Rideshare	600
CMI4	Rideshare	500
CMI5	Rideshare	900

Table 1: Reported sources of income participants and the self-estimated daily income in Baht (approximately 34 Baht corresponds to 1 USD). The DriverID contains an abbreviation for their location (BKK for Bangkok and CMI for Chiang Mai).

To ensure we captured data before, during, and after the peak pollution season, the experiment was conducted from November 1, 2023, to May 15, 2024, covering 197 days (nearly seven months). On the first day, we delivered equipment and set up the MSNs for all riders at both sites simultaneously. Riders followed their regular

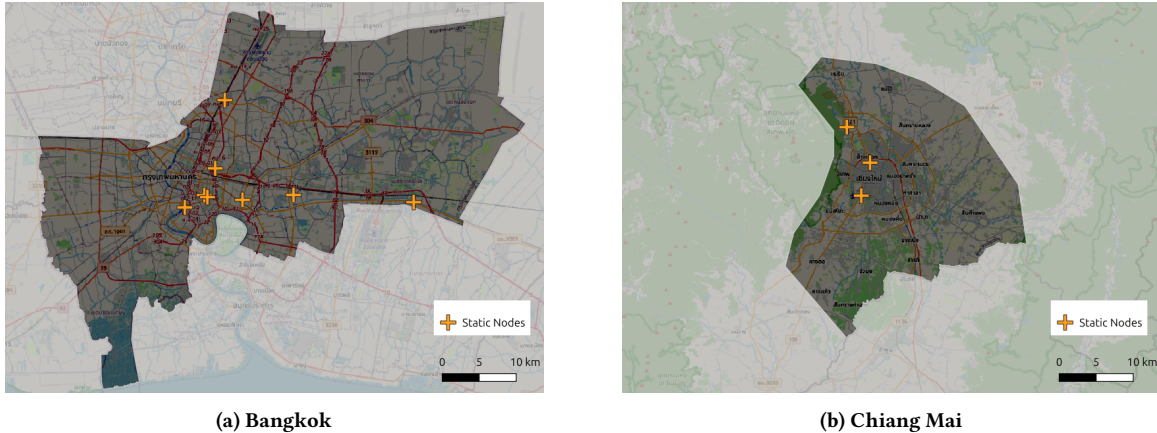


Figure 6: Map of the study areas in Bangkok (a) and Chiang Mai (b), highlighting key routes and locations where MobileSense data was collected as well as locations of static sensor nodes.

work schedules and routes organically throughout the experiment. Every two to three weeks, they were asked to meet with our team for equipment checks and discussions about their recent activities. To compensate for their participation, each rider received 30 USD per week.

The measurements focused on pollution exposure during the riders' working hours, with each rider instructed to activate the sensor at the start of their shift and deactivate it upon finishing. Data was collected at a frequency of 1 Hz, capturing one data sample per second to ensure high-resolution tracking of air pollution exposure throughout their routes.

6 Results

In this section, we first evaluate the reliability of the MobileSense platform by analyzing the uptime and downtime of each Mobile Sensing Node (MSN) throughout the measurement campaign. Next, we examine the distribution of PM_{2.5} concentrations collected from both cities, identifying and filtering out outliers. We then compare the daily PM_{2.5} exposure against the recommended threshold and static node readings. The temporal distribution of exposure is also analyzed to identify peak pollution periods during the day. Finally, we calculate the Hazard Quotient proposed by USEPA to assess the health risks faced by each frontline rider.

6.1 System Reliability Analysis

This section aims to analyze the reliability of our system by measuring the uptime and downtime periods that occur throughout the day. To perform this measurement, we utilized the centralized notification system described in subsection 3.4, as it accounts for all factors contributing to downtime, such as intentional shutdowns during breaks, unexpected system failures, and network disconnections. The notification system sends two types of messages to the riders: Up and Down messages.

Note that two consecutive Up or Down messages are not possible because the state of all sensors deployed in the study area is managed by the centralized notification system. This system monitors the sensor's data transmission status and assigns the Up or Down

state based on a two-minute window. If the sensor continuously transmits data for two minutes after a period of inactivity, it is considered Up. Conversely, if the sensor remains inactive for two minutes, it is classified as Down. If an Up message is followed by a Down message, the time interval between these two messages is considered Uptime. Conversely, if a Down message is followed by an Up message, it is classified as Downtime. The maximum downtime duration for each day is excluded from the analysis, as it indicates that the rider is off work.

Figure 7 presents a plot of the average system uptime and downtime frequency observed throughout the day. Among the boxes, BKK2 and CMI4 stand out with the highest uptime percentages, achieving 98% and 95%, respectively, indicating strong reliability of the system. In contrast, BKK3 and CMI1 exhibit lower uptime rates of 82% and 80%, potentially impacting the volume of data collected from these units. This reduced uptime is linked to their high frequency of downtime occurrences; as shown in the plot, BKK3 and CMI1 experience downtime approximately 3 and 3.5 times per day, respectively.

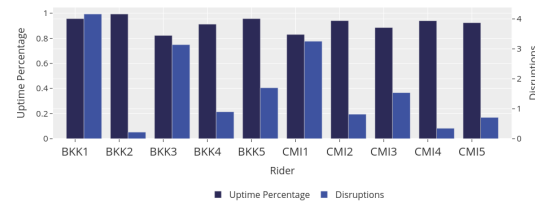


Figure 7: Average uptime percentage of each rider over 7 months measurement period

To investigate the impact of downtime, we measured the recovery time, defined as the interval between when a node goes offline and when it comes back online. This metric provides insight into the responsiveness of both the notification system and the troubleshooting process. The distribution of recovery times is shown in

a box plot in Figure 8. Although recovery times for all boxes exhibit a negatively skewed distribution with some long-tail outliers, the average recovery time remains relatively low, indicating generally quick recovery or effective mitigation strategies. For example, despite experiencing the highest downtime frequency at 4.25 times per day, the BKK1 box has a median recovery time of only 4.54 minutes. This aligns with our troubleshooting procedure outlined in subsection 3.4, where riders are advised to wait 5 minutes after receiving a notification, as temporary disconnections can occur due to cell site handovers. If recovery time exceeds 5 minutes, riders are instructed to check the battery and cable connections before manually resetting the system, which may take additional time. For instance, BKK5 has a low recovery time (14.28 minutes), suggesting swift recovery compared to others, such as CMI4, with a recovery time of 110.61 minutes. Notice that, during the measurement period, CMI4 was awaiting replacement, contributing to its extended recovery time. Another contributing factor to downtime is the breaks riders take during their workday, such as lunchtime, during which downtime was consistently observed across all riders.

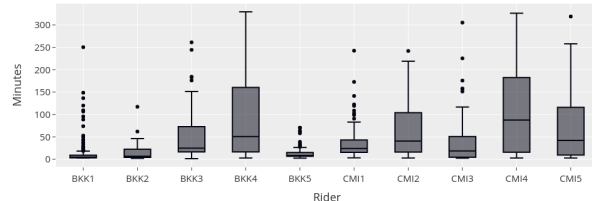


Figure 8: Boxplot showing the distribution of recovery times, highlighting the median, quartiles, and potential outliers in the data.

6.2 Distribution of PM_{2.5} Concentrations

During a 7-month period, more than 50 million PM_{2.5} samples (n) were collected from Bangkok and Chiang Mai. The distribution of PM_{2.5} concentrations in both cities is shown in Figure 12. Figure 9a presents the Probability Density Function (PDF) for PM_{2.5} levels, which range from 0 to 3708 $\mu\text{g}/\text{m}^3$. The most commonly observed concentrations are 31.01 and 20.01 $\mu\text{g}/\text{m}^3$ for Bangkok and Chiang Mai respectively. Figure 9b shows the Cumulative Distribution Function (CDF) of PM_{2.5} concentrations measured in Bangkok and Chiang Mai. The distributions indicate that PM_{2.5} concentrations exceed 15 $\mu\text{g}/\text{m}^3$ with probabilities of 0.93 in Bangkok and 0.91 in Chiang Mai, respectively.

Although the PM_{2.5} sensor (PMS7003) can measure concentrations greater than 1000 $\mu\text{g}/\text{m}^3$, the recommended measurement range is 0 to 500 $\mu\text{g}/\text{m}^3$. Therefore, we applied a 500 $\mu\text{g}/\text{m}^3$ cut-off point to exclude outliers from our data set. As shown in Figure 9b, the probability that PM_{2.5} readings exceed this cut-off point in both Bangkok and Chiang Mai is very low.

6.3 Average Daily PM_{2.5} Exposure

To assess participants' PM_{2.5} exposure during working hours, we collected continuous measurements from the start to the end of

each rider's shift, restricted to periods spent outdoors, primarily while riding. For comparison, we reference data from static sensors (Figures 6a and 6b) equipped with identical PM_{2.5} sensing technology as the MobileSense nodes to minimize measurement bias. Static sensor readings are averaged over 6:00 a.m. to 8:00 p.m., corresponding to the riders' typical working hours.

Figure 10 presents the average daily PM_{2.5} exposure recorded by each rider (individual dots). To facilitate comparison with static sensors located in Bangkok and Chiang Mai, riders' daily exposures are averaged and depicted with dashed lines, alongside the daily averages from the respective static sensors shown as solid lines.

The data indicate that average PM_{2.5} levels measured by riders during their shifts were consistently higher than those recorded by static sensors over the same 6 a.m.–8 p.m. period. In Bangkok, rider-based (mobile sensor) measurements exceeded those from static sensors even during November and December, typically considered a non-critical pollution period. During this time, static sensor readings largely remained below 50 $\mu\text{g}/\text{m}^3$, whereas mobile sensor measurements frequently approached to 100 $\mu\text{g}/\text{m}^3$. This disparity widened from January to February, corresponding to the peak PM_{2.5} season in Bangkok. Notably, on 30 January 2024, the highest rider-based average PM_{2.5} exposure was recorded at 133.8 $\mu\text{g}/\text{m}^3$, compared to 88.1 $\mu\text{g}/\text{m}^3$ from static sensors. Although PM_{2.5} levels in Bangkok began to decline from March onwards, mobile sensor readings continued to remain significantly elevated relative to the static sensor measurements.

In contrast to Bangkok, PM_{2.5} patterns in Chiang Mai exhibit a different trend. From November to March, average PM_{2.5} levels recorded by mobile sensors closely tracked those measured by static sensors. However, during April and May, mobile sensor readings fell below those from the static nodes. Even on the peak pollution day, 6 April 2024, when static sensors recorded an average PM_{2.5} concentration of 283.3 $\mu\text{g}/\text{m}^3$, the corresponding mobile sensor average was notably lower at 219.6 $\mu\text{g}/\text{m}^3$.

All mobile and static sensor nodes employed in this study used the PMS7003 PM_{2.5} sensor, which is known for its strong unit-to-unit consistency [10]. Thus, discrepancies between rider exposure measurements and static sensor readings are unlikely to stem from sensor variability. In Bangkok, elevated PM_{2.5} levels recorded by mobile nodes are mainly attributable to on-road vehicle emissions [24], as riders spent extended periods in traffic-dense areas, close to emission sources. In contrast, static sensors were generally located away from major roadways, which likely contributed to lower PM_{2.5} measurements.

In Chiang Mai, PM_{2.5} measurements from mobile sensors generally aligned with those from static sensors, reflecting the relatively low contribution of on-road vehicle emissions in the area. However, March and April correspond to the typical harvesting period, which involves extensive crop residue burning and forest fires. As a result, PM_{2.5} concentrations rose sharply to hazardous levels, consistent with annual patterns. Interviews with riders indicated that, during this period, they often minimized outdoor exposure by staying indoors during breaks. Additionally, some riders took days off while leaving their sensor nodes operational. These behavioral factors likely contributed to greater variability in mobile measurements and help explain why mobile sensor data occasionally fell below static sensor readings.

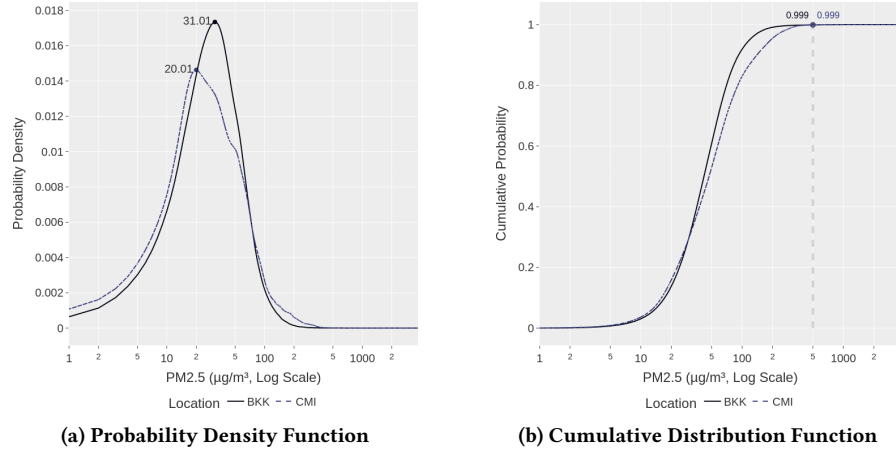


Figure 9: Probability Density Function (a) and Cumulative Distribution Function (b) illustrating the distribution of pollution exposure of all riders in Bangkok (BKK) and Chiang Mai (CMI).

The extent of these daily exposures for individual riders is further illustrated in Figure 11. The box plots summarize the PM_{2.5} concentrations experienced daily by each participant over the 7-month period. Crucially, the figure highlights that the daily PM_{2.5} exposure for all riders in both Bangkok and Chiang Mai consistently exceeded World Health Organization's Air Quality Guidelines (AQG) of 15 $\mu\text{g}/\text{m}^3$ [26], which is indicated by a reference line on the plot. Secondly, the riders at Chiang Mai experience a higher maximum PM_{2.5} exposure compared to Bangkok.

The use of mobile sensors offers significant advantages as it directly measures the riders' actual exposure in real-time, capturing personal exposure levels that may differ from general air quality trends. In contrast, data from static nodes or government-operated reference air quality stations serve as a valuable baseline, providing an overall view of the city's pollutant levels but without capturing individual exposure variations.

6.4 Temporal Distribution

This subsection analyzes the temporal distribution of PM_{2.5} concentrations. Figures 12a and 12b depict the diurnal patterns of average PM_{2.5} concentrations in Bangkok and Chiang Mai, respectively. The data spans the hours from 6 a.m. to 8 p.m., corresponding to the working hours of our volunteer riders. These patterns provide insights into pollution exposure during different times of the day.

In Bangkok, the highest PM_{2.5} levels consistently occur during the early morning hours (6 a.m. - 8 a.m.), particularly in January 2024. The peak value is observed at 7 a.m. in January 2024 (106.34 $\mu\text{g}/\text{m}^3$), indicating significant pollution likely caused by traffic during rush hours. PM_{2.5} levels begin to decline from 9 a.m. onwards and remain stable during the afternoon (12 - 3 p.m.). However, they start rising again after 4 p.m. January experienced the highest pollution levels, with a peak of 106.34 $\mu\text{g}/\text{m}^3$ at 7 a.m. This is due to seasonal effects, such as winter inversion, where air ventilation is limited.

Similarly, in Chiang Mai, PM_{2.5} levels are rising in the early morning hours (6 a.m. - 10 a.m.). The levels then gradually decrease during midday (10 a.m. - 2 p.m.) before rising again in the evening

(4 - 8 p.m.). Both March and April are considered the most polluted months, with consistently high levels throughout the day. A peak value of 183.73 $\mu\text{g}/\text{m}^3$ was recorded at 9 a.m. in March. This aligns with the annual "burning season," during which crop residue burning significantly contributes to air pollution.

The key observation from this analysis is the difference in diurnal patterns during peak pollution periods. In Chiang Mai (March and April), PM_{2.5} levels remain consistently high throughout the day, whereas in Bangkok (January), PM_{2.5} levels peak during specific hours and then decline to levels comparable to other months.

6.5 Health Risk Assessment

To further investigate the impact of PM_{2.5} on human health, we adopted the standardized USEPA human health risk assessment framework for non-cancer effects [25]. This framework evaluates the ratio of exposure to toxicity, commonly referred to as the Hazard Quotient (HQ). The HQ is influenced by factors such as exposure frequency, duration, and pollutant concentration. An HQ value less than 1 indicates a low risk of adverse health effects, whereas an HQ value greater than 1 suggests a higher likelihood of non-carcinogenic health impacts.

$$HQ = \frac{EC}{RfC} \quad (1)$$

Here, RfC denotes the inhalation reference concentration, which serves as a threshold for acceptable exposure. According to the World Health Organization's Air Quality Guidelines (AQG), the average exposure to PM_{2.5} should not exceed 15 $\mu\text{g}/\text{m}^3$ [26]. Therefore, the RfC is set at 15 $\mu\text{g}/\text{m}^3$. The EC (Exposure Concentration) represents the estimated concentration of pollutants inhaled through the respiratory system, expressed in units of $\mu\text{g}/\text{m}^3$. It is calculated using the following equation:

$$EC = \frac{CA \times ET \times EF \times ED}{AT} \quad (2)$$

In this equation:

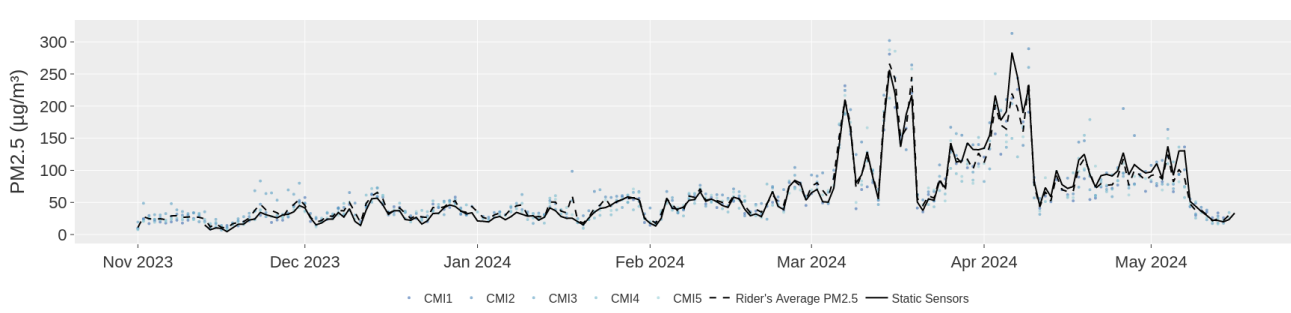
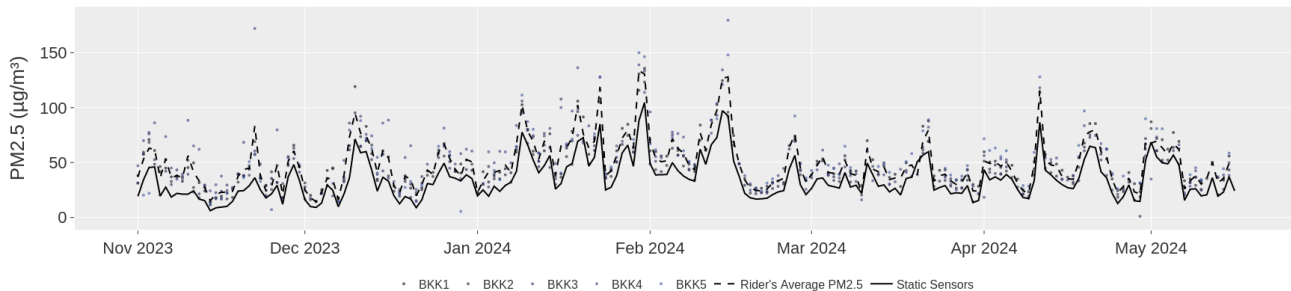


Figure 10: Comparison of data on particulate matter concentration reported by Static Sensors versus data collected by riders in Bangkok (a) and Chiang Mai (b). The analysis reveals that the PM_{2.5} exposure experienced by riders typically exceeds the levels reported by static stations.

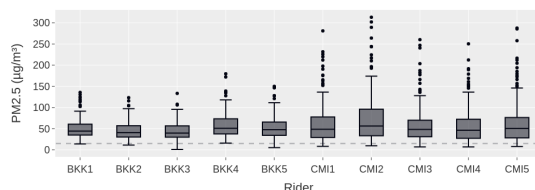


Figure 11: Daily measurements conducted over a 7-month period for all riders in both BKK and CMI, exceeds World Health Organization's Air Quality Guidelines (AQG) of 15 µg/m³.

- CA is the concentration of air pollutants ($\mu\text{g}/\text{m}^3$), determined by the average daily PM_{2.5} exposure for an individual.
- ET is the exposure time (hours/day), representing the average number of hours an individual is exposed per day.
- EF is the exposure frequency (days/year), based on the total working days in a year.
- ED is the exposure duration (years), corresponding to the estimated working years.

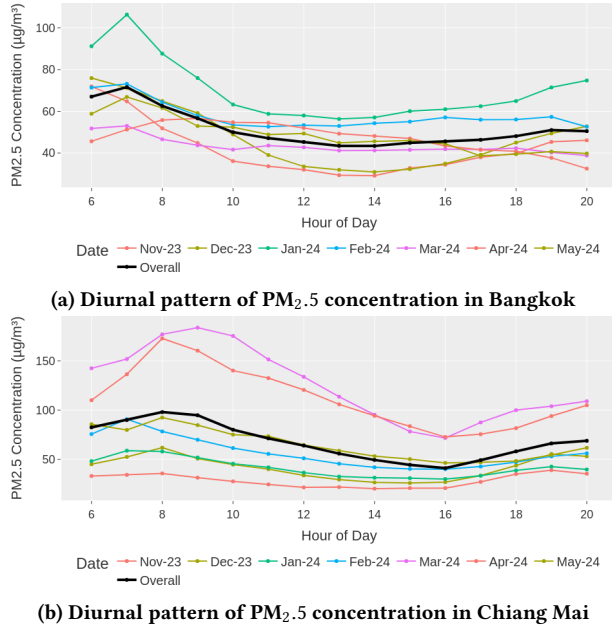
- AT is the average time, calculated as $ED \times 365 \text{ days/year} \times 24 \text{ hours/day}$.

Table 2 presents the exposure values collected from each rider over the 7-month measurement period. The CA values range from 44.5 to 75.47 $\mu\text{g}/\text{m}^3$. The ET parameter was derived from the average working hours per day, which varied between 6.23 and 13.86 hours. The EF parameter was calculated based on the total number of working days during the 7-month period (197 days). The ED parameter was estimated under the assumption that each rider would continue in this occupation for a duration of 10 years.

The result revealed that 6 out of 10 riders exhibited HQ values greater than 1, indicating a high health risk for riders in both Bangkok and Chiang Mai. To determine the key parameters that affect the Hazard Quotient (HQ), we evaluate the relationship between HQ and other factors including PM_{2.5} Concentration (CA), Exposure Time(ET),and Exposure Frequency (EF). The correlation between HQ - CA, HQ - ET and HQ - EF are 0.35, 0.80 and 0.85 respectively. The Exposure Time and Exposure Frequency are the key parameters affecting the Hazard Quotient (HQ), while the PM_{2.5} concentration shows less correlated with HQ. This finding highlights the importance of reducing exposure duration and frequency

Parameters	Unit	BKK1	BKK2	BKK3	BKK4	BKK5	CMI1	CMI2	CMI3	CMI4	CMI5
PM _{2.5} Concentration (CA)	($\mu\text{g}/\text{m}^3$)	50.61	44.50	43.51	56.12	53.91	63.47	75.47	58.16	58.17	64.10
PM _{2.5} Concentration from static sensor (CA_{static})	($\mu\text{g}/\text{m}^3$)	35.1	35.1	35.1	35.1	35.1	60.8	60.8	60.8	60.8	60.8
Exposure Time (ET)	(hours/day)	13.86	11.07	8.45	9.99	8.72	8.49	9.68	6.46	6.23	9.47
Exposure Frequency (EF)	(days/year)	359	321	252	276	219	309	298	272	263	321
Exposure Duration (ED)	(years)	10	10	10	10	10	10	10	10	10	10
Average Time (AT)	(hours)	87600	87600	87600	87600	87600	87600	87600	87600	87600	87600
Working Days	(days)	194	173	136	149	118	167	161	147	142	173
Hazard Quotient (HQ)	-	1.92	1.2	0.71	1.18	0.78	1.27	1.66	0.78	0.73	1.43
Hazard Quotient calculated from static sensor (HQ_{static})	-	1.33	0.95	0.57	0.74	0.51	1.21	1.34	0.81	0.76	1.41

Table 2: Exposure Factors and Hazard Quotient Calculation

Figure 12: Hourly trends of PM_{2.5} exposure during work hours in (a) Bangkok and (b) Chiang Mai.

to minimize health risks for riders. Furthermore, the results presented in Table 2 show that riders working more than 8.49 hours per day or 276 days per year consistently exhibited HQ values greater than 1. It is important to note that this assessment considers only PM_{2.5} exposure. In reality, these riders are exposed to additional pollutants, which could further elevate their HQ value.

Furthermore, we examine the scenario in which exposure assessment relies solely on static sensors. To this end, we select static sensor stations located closest to the participants' daily routes in Bangkok and Chiang Mai. The selected sensors are situated in the city centers, representing common points traversed by all riders during their daily commutes. The average air pollution concentrations measured by these static nodes, denoted as CA_{static} , are 35.1 $\mu\text{g}/\text{m}^3$

and 60.8 $\mu\text{g}/\text{m}^3$ for Bangkok and Chiang Mai, respectively. The corresponding hazard quotients, HQ_{static} , are reported in Table 2. In comparison to the hazard quotients derived from mobile sensor data, notable differences are observed. The number of high-risk riders, defined as those with hazard quotients exceeding 1, decreases from 6 to 4 when using static sensor measurements. Specifically, in Bangkok, the number of high-risk riders declines from 3 to 1, whereas in Chiang Mai, it remains as 3. These discrepancies underscore that reliance on static sensor data alone is insufficient to accurately assess individual health risks, highlighting the critical importance of mobile monitoring in exposure evaluation.

To mitigate the high values of HQ, we simulated scenarios in which the Exposure Frequency (EF) and Exposure Duration (ED) were minimized using the following strategies:

1-Hour Break: In this strategy, riders take a one-hour break during peak pollution hours each day. This one-hour break is applied daily throughout the seven-month period. Based on the diurnal pollution pattern shown in Figure 12, the average peak pollution periods over a seven-month period were 7:00–8:00 a.m. in Bangkok and 8:00–9:00 a.m. in Chiang Mai. The one-hour break is implemented daily throughout the seven-month period.

Full Days Off on Consecutive Days: This strategy recommends that riders take multiple full days off over consecutive days when PM_{2.5} levels are at their highest. We tested scenarios where riders took 3, 5, or 7 consecutive days off.

Full Days Off on Selected Peak Days: Similar to the previous strategy, this approach suggests taking full days off, but instead of consecutive days, the breaks are distributed across the most polluted days, which may not occur in a continuous sequence.

Based on the results presented in Figure 10 and Figure 12, the 1-hour break and days-off periods were selected for Bangkok and Chiang Mai, as detailed in Table 3. To apply these strategies, the collected PM_{2.5} samples were excluded according to the chosen period, and the other exposure factors including CA, ET and EF were recalculated accordingly.

Figure 13 illustrates the reduction in the Hazard Quotient (HQ) achieved by various mitigation strategies, compared to the baseline HQ obtained from measurements. Overall, the 7-Day Peak strategy is the most effective, reducing HQ values by 7.17% (BKK3) to 15.01% (CMI1). Conversely, the full days off on consecutive days strategy is

Strategies	Bangkok	Chiang Mai
1-Hour Break (1 Hour)	7:00–8:00 a.m. daily	8:00–9:00 a.m. daily
Full Days Off on 3 Consecutive Days (3-Day Con)	30 Jan to 1 Feb	14 Mar to 16 Mar
Full Days Off on 3 Selected Peak Days (3-Day Peak)	30 Jan, 31 Jan, 15 Feb	15 Mar, 16 Mar, 19 Mar
Full Days Off on 5 Consecutive Days (5-Day Con)	29 Jan to 2 Feb	13 Mar to 17 Mar
Full Days Off on 5 Selected Peak Days (5-Day Peak)	23 Jan, 30 Jan, 31 Jan, 14 Feb, 15 Feb	7 Mar, 15 Mar, 16 Mar, 19 Mar, 6 Apr
Full Days Off on 7 Consecutive Days (7-Day Con)	28 Jan to 3 Feb	12 Mar to 18 Mar
Full Days Off on 7 Selected Peak Days (7-Day Peak)	9 Jan, 19 Jan, 23 Jan, 30 Jan, 31 Jan, 14 Feb, 15 Feb	7 Mar, 15 Mar, 16 Mar, 19 Mar, 3 Apr, 6 Apr, 7 Apr

Table 3: Selected Period for Implemented Mitigation Strategies

less effective. When comparing strategies with the same number of days off, the full days off on peak days consistently outperforms the consecutive days approach. Additionally, the 5-Day Peak strategy results in a greater HQ reduction than the 7-Day Consecutive (7-Day Con) strategy for nearly all riders.

On the other hand, the 1-Hour Break strategy proves highly effective for most riders in Bangkok. For instance, riders BKK1 and BKK4 experience significant HQ reductions of 8.26% and 7.64%, respectively, indicating that reducing exposure by just one hour daily is particularly beneficial for them. This suggests that pollution exposure in Bangkok is more concentrated during specific hours (e.g., peak traffic times), making even a short reduction in exposure (1 hour) highly impactful. Moreover, Bangkok riders typically face peak PM_{2.5} exposure during high-traffic hours, so reducing work hours results in a greater relative decrease in HQ. In contrast, Chiang Mai experiences more evenly distributed pollution levels throughout the day, particularly during the burning season (March–April). As a result, the 1-Hour Break strategy is less effective compared to taking full days off. An exception is rider BKK5, who does not benefit from the 1-Hour Break strategy. This is because BKK5 starts working after the peak pollution period, making the one-hour reduction ineffective in lowering exposure.

If the 1-Hour Break strategy is implemented, the estimated economic loss over the 7-month period would be 652.21 USD for the Bangkok rider and 393.45 USD for the Chiang Mai rider. These losses are calculated by multiplying the hourly wage by the number of average working days (154 days for Bangkok and 158 days for Chiang Mai).

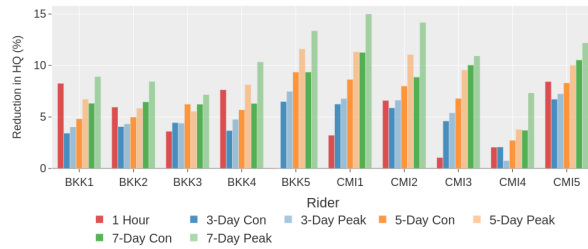
In comparison, the 7-Day Off strategy would result in a lower economic loss of 308.82 USD for Bangkok riders and 140.00 USD for Chiang Mai riders, making it a more cost-effective option than the 1-Hour Break strategy.

This economic perspective is crucial for assessing the feasibility and impact of different mitigation strategies. Ultimately, each rider can select the most suitable approach based on their work routine, balancing health benefits and economic loss.

7 Discussion

We developed MobileSense, a low-cost mobile sensing platform for real-time air quality monitoring among frontline motorcycle riders. Its goal is to provide an accessible tool for measuring actual personal exposure, particularly for vulnerable groups with limited access to healthcare due to lower income and long working hours. Unlike traditional air pollution data, which rely on stationary monitoring stations often located far from pollution sources, MobileSense captures on-the-ground exposure levels, bridging the gap in accurate human pollution assessment. The platform has demonstrated stability in challenging environments, including extreme heat, rain, and high levels of pollution, which sustains long-term operation. System failures primarily stem from mobile sensing nodes, those include losing Internet connectivity or frequent network handovers due to high-speed driving. Most glitches were automatically resolved through our self-recovery function; otherwise, alerts were sent to riders prompting a hard reset. This was a key reason for developing our own platform instead of relying on off-the-shelf low-cost sensors or IoT devices. By customizing the system, we ensured greater reliability and resilience in real-world conditions. Poor connectivity represents another major obstacle to our measurements, as it occasionally led to temporary disruptions in data transmission. However, this issue has been rarely reported in our measurement. To mitigate the risk of data loss, our nodes were equipped with local storage (a 64 GB SD card). When connectivity was lost, the nodes continued to store data locally and automatically transmitted the buffered data once the connection was restored. This design effectively provides safeguard against data loss due to intermittent connectivity.

However, we have to accept that the MobileSense has limitations in reading accuracy compared to standard air quality stations. As it

**Figure 13: Comparing the improvement in the Hazard Quotient across different mitigation strategies.**

To determine the best mitigation strategy for each city, we must consider economic losses, specifically the daily wages earned by riders. Based on the demographic data in Table 1, Bangkok riders earn approximately 44 USD (1,500 THB) per day, while Chiang Mai riders earn approximately 20 USD (680 THB) per day. The average working hours per day for Bangkok and Chiang Mai riders are 10.41 and 8.06 hours (based on data in Table 2), which allows us to calculate the average hourly wage of both cities as 4.23 USD and 2.48 USD.

relies on low-cost sensor technology, measurement errors typically range between 10% and 15%. To mitigate this effect, MobileSense, like other low-cost sensor platforms, requires calibration and validation against standard equipment, which significantly improves accuracy. Nevertheless, the advantages of low-cost sensors—including affordability, portability, and ease of maintenance—often outweigh minor accuracy limitations. In practice, well-calibrated low-cost sensors effectively detect pollution trends, capturing rising and declining patterns. Additionally, averaging methods help filter out anomalies, ensuring meaningful and actionable data. After weighing this tradeoff, MobileSense remains a viable solution for measuring air pollution in scenarios where standard equipment is not feasible.

It is important to highlight that the data collected from MobileSense has raised significant concerns about the health risks faced by frontline motorcycle riders. Our analysis of daily pollution exposure and health risk assessment consistently indicates that these workers are at high risk. As a mitigation effort, we provided face masks to all participating riders. However, interviews revealed that most of the riders wore masks for only a limited period each day. Many reported that combining a mask with a helmet and face shield made breathing difficult and impaired their ability to work comfortably, thereby limiting the effectiveness of this protective measure. These findings underscore the urgent need for targeted occupational health interventions and adaptive protective strategies tailored to the specific working conditions of mobile outdoor workers in highly polluted urban environments.

Beyond air pollution, we also found that many riders exceed recommended working hours. For instance, a rider in Bangkok worked over 13 hours per day, with only three days off in seven months. Such intense work schedules can lead to long-term health consequences, including chronic stress and fatigue. To address this issue, our study proposes strategies to reduce pollution exposure and improve well-being, such as taking short breaks during the day or scheduling full days off. These measures not only help limit pollution intake but also provide much-needed recovery time. However, implementation is challenging, as many riders prioritize income over health. We hope this study serves as a catalyst for engaging government agencies, such as the Ministry of Labor and the Ministry of Public Health, to develop policies that protect this vulnerable workforce.

8 Conclusion

This paper presents MobileSense, a low-cost mobile sensor platform designed to monitor air pollution exposure among outdoor workers, particularly motorcycle riders in urban areas. Over the course of a seven-month field study in Bangkok and Chiang Mai, MobileSense successfully collected real-time PM_{2.5} data, offering critical insight into riders' personal exposure levels. Our findings reveal that PM_{2.5} exposure measured by mobile sensors is significantly higher than that recorded by low-cost static sensors deployed in the cities. As a result, motorcycle riders experience extreme PM_{2.5} exposure, exceeding WHO-recommended limits, even during low-pollution seasons. To assess the associated health risks, we applied the Hazard Quotient (HQ) method proposed by the USEPA, which classified 6 out of 10 riders as high-risk. To mitigate these risks,

we propose three exposure reduction strategies; 1)A daily 1-hour break during peak pollution hours, 2) Full days off on consecutive high-pollution days (3, 5, or 7 days), and 3) Full days off on peak pollution days, which , which do not necessarily have to be consecutive. As is widely recognized, the most sustainable approach to minimizing exposure is the reduction of PM_{2.5} concentrations. However, achieving substantial reductions remains challenging. Therefore, limiting exposure duration and frequency is crucial for mitigating health risks among riders. Our analysis suggests that the 1-hour break strategy is more effective for Bangkok riders due to pollution being concentrated during peak hours. In contrast, taking full days off on peak pollution days is more suitable for Chiang Mai riders, where pollution levels remain consistently high throughout the day.

For future research, we aim to perform high-resolution spatial analyses of PM_{2.5} concentrations to identify and map pollution hotspots across both cities, providing a foundation for targeted mitigation strategies. We also plan to further advance MobileSense's capabilities, enabling broader deployment across a range of high-risk occupational groups and urban environments, particularly in developing countries where air quality monitoring remains limited. Moreover, we envision integrating medical evaluations into our study by conducting longitudinal health assessments of our volunteer cohort, offering critical insights into the long-term impacts of chronic air pollution exposure.

Acknowledgments

This research was supported by the National Science Foundation (NSF) under Grant No. 2025022, which we gratefully thank for their support. Additionally, we used generative AI tools to assist with proofreading and improving the clarity of the English writing.

References

- [1] Thongchai Kanabkaew Achara Taweesan, Adisorn Lertsinsubtavee. 2022. Understanding the Rapid Change of PM_{2.5} Using Low-cost Air Quality IoT Sensors. In *INTERNATIONAL CONFERENCE ON GREEN TECHNOLOGY AND DESIGN (ICGTD)*.
- [2] Mushtaq Ahmad, Thanaphum Manjanarat, Wachiraya Rattanawongs, Phitchaya Muensri, Rattaporn Saenmuangchin, Annop Klamcon, Sasitorn Aueviriyavat, Kanokwan Sukrak, Wiyong Kangwansupamonkon, and Sirima Panyametheekul. 2022. Chemical Composition, Sources, and Health Risk Assessment of PM_{2.5} and PM₁₀ in Urban Sites of Bangkok, Thailand. *International Journal of Environmental Research and Public Health* 2022, Vol. 19, Page 14281 19 (11 2022), 14281, Issue 21. <https://doi.org/10.3390/IJERPH192114281>
- [3] AIRPARIF. 2023. *AIRLAB Microsensors Challenge 2023 Protocol*. Technical Report.
- [4] AirVisual Outdoor | Air quality monitor [n. d.]. <https://www.iqair.com/th-en/products/air-quality-monitors/airvisual-outdoor-2-pm>
- [5] Mohammad Ehsanul Alim, Sarosh Ahmad, Marzieh Naghd Dorabati, and Ihab Hassoun. 2020. Design & Implementation of IoT Based Smart Helmet for Road Accident Detection. In *2020 11th IEEE Annual Information Technology, Electronics and Mobile Communication Conference (IEMCON)*. 0576–0581. <https://doi.org/10.1109/IEMCON51383.2020.9284821>
- [6] Joshua S. Apte, Kyle P. Messier, Shahzad Gani, Michael Brauer, Thomas W. Kirchstetter, Melissa M. Lunden, Julian D. Marshall, Christopher J. Portier, Roel C.H. Vermeulen, and Steven P. Hamburg. 2017. High-Resolution Air Pollution Mapping with Google Street View Cars: Exploiting Big Data. *Environmental Science & Technology* 15, 12 (June 2017). <https://doi.org/10.1021/acs.est.7b00891>
- [7] Marek Badura, Piotr Batog, Anetta Drzeniecka-Osiadacz, and Piotr Modzel. 2018. Evaluation of Low-Cost Sensors for Ambient PM_{2.5} Monitoring. *Journal of Sensors* 2018, 1 (2018), 5096540. <https://doi.org/10.1155/2018/5096540> arXiv:<https://onlinelibrary.wiley.com/doi/pdf/10.1155/2018/5096540>
- [8] Petra Bauerová, Adriana Šindelářová, Štěpán Rychlík, Zbyněk Novák, and Josef Keder. 2020. Low-Cost Air Quality Sensors: One-Year Field Comparative Measurement of Different Gas Sensors and Particle Counters with Reference Monitors at Tušimice Observatory. *Atmosphere* 11, 5 (2020). <https://doi.org/10.3390/atmos1105035>

- //doi.org/10.3390/atmos11050492
- [9] C. J. Behr, A. Kumar, and G. P. Hancke. 2016. A smart helmet for air quality and hazardous event detection for the mining industry. In *2016 IEEE International Conference on Industrial Technology (ICIT)*. 2026–2031. <https://doi.org/10.1109/ICIT.2016.7475079>
- [10] Csörgő Báthory, Zsolt Dobó, Attila Garami, Árpád Palotás, and Pál Tóth. 2022. Low-cost monitoring of atmospheric PM—development and testing. *Journal of Environmental Management* 304 (2022), 114158. <https://doi.org/10.1016/j.jenvman.2021.114158>
- [11] LY Corporation. 2025. Messaging API | LINE Developers. <https://developers.line.biz/en/services/messaging-api/>
- [12] Priyanka deSouza, Amin Anjomshoaa, Fabio Duarte, Ralph Kahn, Prashant Kumar, and Carlo Ratti. 2020. Air quality monitoring using mobile low-cost sensors mounted on trash-trucks: Methods development and lessons learned. *Sustainable Cities and Society* 60 (2020), 102239. <https://doi.org/10.1016/j.scs.2020.102239>
- [13] Nathaniel R. Fold, Mary R. Allison, Berkley C. Wood, Pham T.B. Thao, Sébastien Bonnet, Savitri Garivait, Richard Kamens, and Sithippong Pengjan. 2020. An Assessment of Annual Mortality Attributable to Ambient PM_{2.5} in Bangkok, Thailand. *International Journal of Environmental Research and Public Health* 2020, Vol. 17, Page 7298 17 (10 2020), 7298. Issue 19. <https://doi.org/10.3390/IJERPH17197298>
- [14] Ghaida, Azka, Firdaus, Fadhil Muhammad, Qatrunnada, Khalisha Meliana, Peters, Daniel, Cardenas, Beatriz, and Lestari, Puji. 2024. Spatial patterns of PM_{2.5} air pollution in Jakarta: Insights from mobile monitoring. *E3S Web of Conf.* 485 (2024), 06002. <https://doi.org/10.1051/e3sconf/202448506002>
- [15] Nguyen Nhat Ha Chi and Nguyen Thi Kim Oanh. 2021. Photochemical smog modeling of PM_{2.5} for assessment of associated health impacts in crowded urban area of Southeast Asia. *Environmental Technology & Innovation* 21 (2021), 101241. <https://doi.org/10.1016/j.eti.2020.101241>
- [16] Aswin Giri J. and Shiva Nagendra S.M. 2023. Spatio-temporal exposure assessment of particulate matter pollution in auto-rickshaw drivers in Chennai, India. *Atmospheric Pollution Research* 14, 12 (2023), 101933. <https://doi.org/10.1016/j.apr.2023.101933>
- [17] Sobia Kausar, Phanika Tongchai, Sumed Yadoung, Shamsa Sabir, Supansa Pata, Wootitchai Khamduang, Kriangkrai Chawansuntati, Supachai Yodkeeree, Anurak Wongta, and Surat Hongsibsong. 2024. Impact of fine particulate matter (PM_{2.5}) on ocular health among people living in Chiang Mai, Thailand. *Scientific Reports* 2024 14:1 14 (11 2024), 1–10. Issue 1. <https://doi.org/10.1038/s41598-024-77288-8>
- [18] Dohyeong Kim, Yunjin Yum, Kevin George, Ji-Won Kwon, Woo Kyung Kim, Hey-Sung Baek, Dong In Suh, Hyeon-Jong Yang, Young Yoo, Jinho Yu, Dae Hyun Lim, Sung-Chul Seo, and Dae Jin Song. 2021. Real-Time Low-Cost Personal Monitoring for Exposure to PM_{2.5} among Asthmatic Children: Opportunities and Challenges. *Atmosphere* 12, 9 (2021). <https://doi.org/10.3390/atmos12091192>
- [19] Wissanupong Kliengchuay, Sarima Niampradit, Narut Sahanavin, Anurak Mueller, Susanne Steinle, Miranda Loh, Helinor Jane Johnston, Sotiris Vardoulakis, San Suwanmanee, Walaiporn Phonphan, John W. Cherrie, and Kraichat Tantrakarnapa. 2025. Seasonal analysis of indoor and outdoor ratios of PM_{2.5} and PM₁₀ in Bangkok and Chiang Mai: A comparative study of haze and non-haze episodes. *Heliyon* 11, 3 (2025), e42261. <https://doi.org/10.1016/j.heliyon.2025.e42261>
- [20] Adisorn Lertsinsrubtavee, Kalana Gayashan Sarambage Jayarathna, Preechai Mekbungwan, Thongchai Kanabkaew, and Sunee Raksakietisak. 2022. SEA-HAZEMON: Active Haze Monitoring and Forest Fire Detection Platform. In *Proceedings of the 17th Asian Internet Engineering Conference* (Hiroshima, Japan) (AINTEC '22). Association for Computing Machinery, New York, NY, USA, 88–95. <https://doi.org/10.1145/3570748.3570761>
- [21] SIMCom Wireless Solutions Limited. 2024. SIM7600X-H-M2. <https://www.simcom.com/product/SIM7600X-H-M2.html>
- [22] MQTT.org. 2024. MQTT - The Standard for IoT Messaging. <https://mqtt.org/>
- [23] Raunak Mukhia, Kalana Gayashan Sarambage Jayarathna, and Adisorn Lertsinsrubtavee. 2023. Performance Evaluation of LoRaWAN Forest Fire Monitoring Network in the Wild. In *Proceedings of the 18th Asian Internet Engineering Conference* (Hanoi, Vietnam) (AINTEC '23). Association for Computing Machinery, New York, NY, USA, 96–104. <https://doi.org/10.1145/3630590.3630602>
- [24] Daiju Narita, Nguyen Thi Kim Oanh, Keiichi Sato, Mingjun Huo, Didin Agustian Permadi, Nguyen Nhat Ha Chi, Tanatrat Ratanajaratroj, and Ittipol Pawarmart. 2019. Pollution Characteristics and Policy Actions on Fine Particulate Matter in a Growing Asian Economy: The Case of Bangkok Metropolitan Region. *Atmosphere* 10, 5 (April 2019). <https://doi.org/10.3390/atmos10050227>
- [25] Office of Superfund Remediation and Technology Innovation Environmental Protection Agency. 2009. *Risk Assessment Guidance for Superfund Volume I: Human Health Evaluation Manual (Part F, Supplemental Guidance for Inhalation Risk Assessment)*. Technical Report EPA 540-R-070-002. United States Environmental Protection Agency USEPA, Washington, DC 20460.
- [26] World Health Organization. 2021. *WHO global air quality guidelines. Particulate matter (PM_{2.5} and PM₁₀), ozone, nitrogen dioxide, sulfur dioxide and carbon monoxide*. Technical Report ISBN: 9789240034228. WHO.
- [27] PlanTower. 2024. PMS7003—Laser PM_{2.5} Sensor-Plantower Technology. https://plantower.com/en/products_33/76.html
- [28] PurpleAir Zen - Air Quality Monitor [n. d.]. <https://www2.purpleair.com/products/purpleair-zen>
- [29] Bosch Sensortec. 2024. Humidity Sensor BME280. <https://www.bosch-sensortec.com/products/environmental-sensors/humidity-sensors-bme280/>
- [30] Kritika Shukla and Shankar G. Aggarwal. 2022. A Technical Overview on Beta-Attenuation Method for the Monitoring of Particulate Matter in Ambient Air. *Aerosol and Air Quality Research* 22, 12 (2022), 220195. <https://doi.org/10.4209/aaqr.220195>
- [31] Yuxi Sun, Peter Brimblecombe, Peng Wei, Yusen Duan, Jun Pan, Qizhen Liu, Qingyan Fu, Zhiqiang Peng, Shuhong Xu, Ying Wang, and Zhi Ning. 2022. High Resolution On-Road Air Pollution Using a Large Taxi-Based Mobile Sensor Network. *Sensors* 22, 16 (2022). <https://doi.org/10.3390/s22166005>
- [32] Espressif Systems. 2023. ESP32WROOM32D & ESP32WROOM32U Datasheet. <https://www.espressif.com/en/support/download/documents>.
- [33] Tin-Tin WIN-SHWE, Zaw Lin THEIN, Win Yu AUNG, Ei Ei Pan Nu YI, Cherry MAUNG, Nay Chi NWAY, Zarli THANT, Takehiro SUZUKI, Ohn MAR, Yang ISHIGAKI, and Daisuke NAKAJIMA. 2020. Improvement of GPS-attached Pocket PM_{2.5} Measuring Device for Personal Exposure Assessment. *Journal of UOEH* 42, 4 (2020), 307–315. <https://doi.org/10.7888/jueh.42.307>
- [34] Winsen. 2024. Electrochemical CO Sensor Module ZE07-CO. <https://www.winsen-sensor.com/sensors/co-sensor/ze07-co.html>
- [35] Winsen. 2024. MH-Z16 NDIR CO₂ SENSOR. <https://www.winsen-sensor.com/sensors/co2-sensor/mh-z16.html>

A Online Resources

The dataset used in this study has been published at the following link: <https://github.com/intERLab-AIT/MobileSenseData>. All participants provided their informed consent, and no personal or identifiable information is displayed about volunteers. All data presented on the platform are fully anonymized and aggregated to ensure participant privacy.